Direct Torque Control of PWM Inverter-Fed AC Motors—A Survey

Giuseppe S. Buja, *Fellow, IEEE,* and Marian P. Kazmierkowski, *Fellow, IEEE*

***Abstract*—This paper presents a review of recently used direct torque and flux control (DTC) techniques for voltage inverter-fed induction and permanent-magnet synchronous motors. A variety of techniques, different in concept, are described as follows: switching-table-based hysteresis DTC, direct self control, constant-switching-frequency DTC with space-vector modulation (DTC-SVM). Also, trends in the DTC-SVM techniques based on neuro-fuzzy logic controllers are presented. Some oscillograms that illustrate properties of the presented techniques are shown.**

***Index Terms*—AC motors, direct torque control (DTC), voltage-source inverters.**

I. Introduction

THE induction motor (IM), thanks to its well-known advantages of simple construction, reliability, ruggedness, and low cost, has found very wide industrial applications. Furthermore, in contrast to the commutation dc motor, it can be used in an aggressive or volatile environment since there are no problems with spark and corrosion. These advantages, however, are superseded by control problems when using an IM in industrial drives with high performance demands. Based on commonly adopted complex space-vector description (represented in a coordinate frame K rotating with angular speed ω_K and written in per-unit form), the IM equations are [8], [10], [36], [40], [77]–[79]

$$\mathbf{u}_{sK} = r_s \mathbf{i}_{sK} + T_N \frac{d\boldsymbol{\psi}_{sK}}{dt} + j\omega_K \boldsymbol{\psi}_{sK} \tag{1}$$

$$0 = r_r \mathbf{i}_{sK} + T_N \frac{d\boldsymbol{\psi}_{rK}}{dt} + j\left(\omega_K - \omega_m\right)\boldsymbol{\psi}_{rK} \tag{2}$$

$$\boldsymbol{\psi}_{sK} = l_s \mathbf{i}_{sK} + l_M \mathbf{i}_{rK} \tag{3}$$

$$\boldsymbol{\psi}_{rK} = l_r \mathbf{i}_{rK} + l_M \mathbf{i}_{sK} \tag{4}$$

$$\frac{d\omega_m}{dt} = \frac{1}{T_M}\left[\mathrm{Im}\left(\boldsymbol{\psi}^*_{sK}\mathbf{i}_{sK}\right) - m_L\right] \tag{5}$$

where $\mathbf{u}_s$, $\mathbf{i}_s$, $\mathbf{i}_r$, $\boldsymbol{\psi}_s$, and $\boldsymbol{\psi}_r$ are the stator voltage, stator current, rotor current, stator flux linkage, and rotor flux linkage vectors, respectively; ω_m is the mechanical angular speed; m_L is the load torque; l_s, l_r, and l_M are the stator, rotor, and magnetizing inductances; $T_N = 1/2\pi 50$ Hz for a nominal frequency of 50 Hz; T_M is the mechanical time constant, and the index K denotes the rotating coordinate system.

Manuscript received June 9, 2003; revised October 20, 2003. Abstract published on the Internet May 20, 2004.

G. S. Buja is with the Department of Electrical Engineering, University of Padova, 35131 Padova, Italy (e-mail: giuseppe.buja@unipd.it).

M. P. Kazmierkowski is with the Institute of Control and Industrial Electronics, Warsaw University of Technology, 00-662 Warsaw, Poland (e-mail: mpk@isep.pw.edu.pl).

Digital Object Identifier 10.1109/TIE.2004.831717

IM control methods can be divided into *scalar* and *vector control*. The general classification of the variable-frequency methods is presented in Fig. 1. In scalar control, which is based on relationships valid in steady state, only magnitude and frequency (angular speed) of voltage, current, and flux linkage space vectors are controlled. Thus, the scalar control does not act on space vector position during transients. Contrarily, in vector control, which is based on relations valid for dynamic states, not only magnitude and frequency (angular speed) but also instantaneous positions of voltage, current, and flux space vectors are controlled. Thus, the vector control acts on the positions of the space vectors and provides their correct orientation both in steady state and during transients. According to the definition above, vector control is a general control philosophy that can be implemented in many different ways. The most popular method, known as *field-oriented control* (FOC) or *vector control*, has been proposed by Hasse [28] and Blaschke [5], and gives the induction motor high performance. In the vector control the motor equations are transformed in a coordinate system that rotates in synchronism with the rotor flux vector. These new coordinates are called *field coordinates*. In field coordinates—under constant rotor flux amplitude—there is a *linear* relationship between control variables and torque. Moreover, like in a separately excited dc motor, the reference for the flux amplitude is reduced in the field-weakening region in order to limit the stator voltage at high speed. Transformation of IM equations in the field coordinates has a good physical basis because it corresponds to the decoupled torque production in a separately excited dc motor. However, from the theoretical point of view, other types of coordinate transformations can be selected to achieve decoupling and linearization of IM equations. This has originated the methods known as modern nonlinear control [6], [61], [73]. Marino *et al.* [53] have proposed a nonlinear transformation of the motor state variables so that, in the new coordinates, the speed and rotor flux amplitude are decoupled by feedback; the method is called *feedback linearization control* (FLC) or *input–output decoupling* [6], [39], [40], [61]. A similar approach, derived from a *multi-scalar* model of the induction motor, has been proposed by Krzeminski [45]. A method based on the *variation* theory and energy shaping has been investigated recently and is called *passivity-based control* (PBC) [60]. In this case, an IM is described in terms of the Euler–Lagrange equations expressed in generalized coordinates.

When, in the mid 1980s, there was a trend toward the standardization of the control systems on the basis of the FOC philosophy, there appeared the innovative studies of Depenbrock [2], [19], [20] and of Takahashi and Noguchi [71], which depart

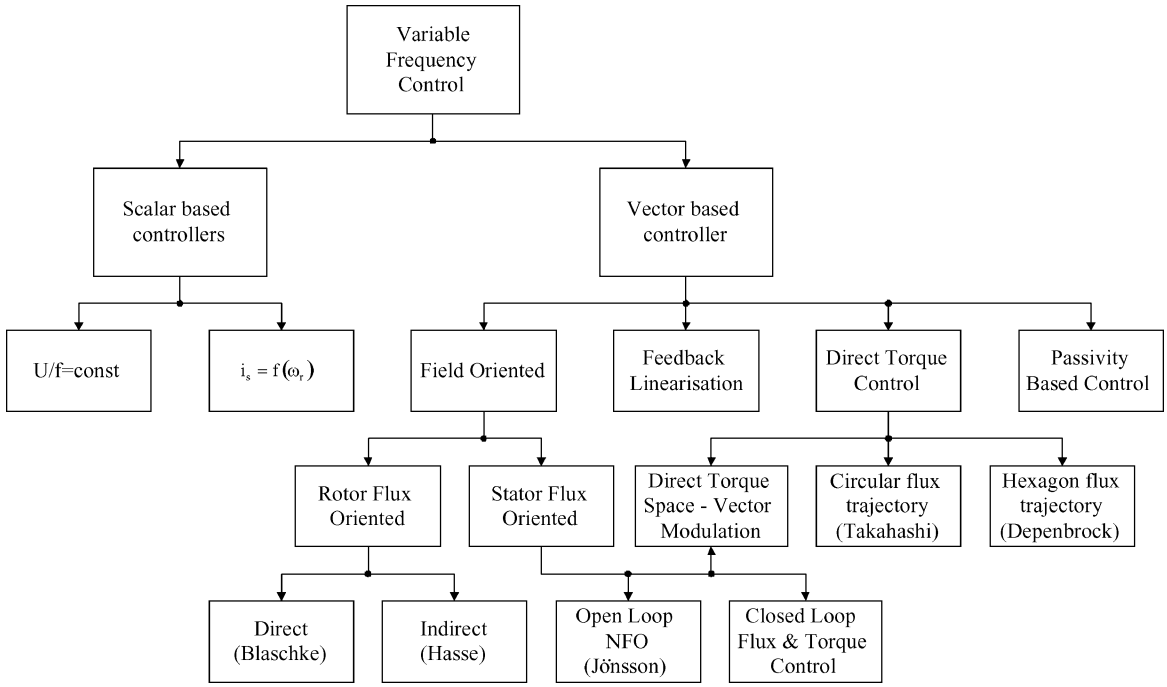

Fig. 1. Classification of IM control methods (NFO—natural field orientation [34], [35]).

from the idea of coordinate transformation and the analogy with dc motor control. These innovators proposed to replace the decoupling control with the bang-bang control, which meets very well with on–off operation of the inverter semiconductor power devices. This control strategy is commonly referred to as *direct torque control* (DTC) and since 1985 it has been continuously developed and improved by many other researchers (see list of references). The purpose of this paper is to give a short review of the available DTC techniques and to put in evidence the differences and peculiarities of each of them. It is devoted basically to the three-phase two-level inverters. However, some references are included concerning multilevel topologies [17].

Remark

Since there is no commonly shared terminology regarding DTC, in this paper under the DTC scheme we refer to control schemes operating with closed torque and flux loops without current controllers.

II. Basic Concepts

A. Basic Principles

In the standard version of FOC schemes, the current component i_{sq} is used as the torque control quantity. Under constant rotor flux amplitude, it adjusts the torque directly as given by

$$m_e = \frac{l_M}{l_r}\psi_r i_{sq} = \frac{l_M}{l_r}\psi_r i_s \sin\delta \tag{6}$$

where m_e is the electromagnetic torque, ψ_r is the rotor flux linkage magnitude, i_s is the stator current magnitude, and δ is the torque angle [Fig. 2(a)]. This makes the current-controlled (CC) pulsewidth-modulation (PWM) inverter [40] very convenient for the implementation of the FOC scheme [Fig. 2(a)]. In the case of voltage-source (VS) PWM inverter-fed IM drives, however, not only the stator current but also the stator flux may be used as the torque control quantity [Fig. 2(b)]

$$m_e = \frac{l_M}{l_r}\psi_r \frac{1}{\sigma l_s}\psi_s \sin\delta_\psi \tag{7}$$

where ψ_S is the stator flux magnitude, δ_ψ is the torque angle, and σ is the leakage factor [Fig. 2(b)]. Note that the stator flux is a state variable, which can be adjusted by stator voltage.

From the stator voltage (1), for $r_s = 0$, it is

$$T_N \frac{d\boldsymbol{\psi}_s}{dt} = \mathbf{u}_s = \mathbf{u}_\nu \tag{8}$$

where $\mathbf{u}_\nu$ is the inverter output voltage vector [Fig. 3(a) and (b)] described by the following equation:

$$\mathbf{u}_\nu = \begin{cases} \left(\frac{2}{3}\right) u_{\rm dc} e^{j(\nu-1)\pi/3}, & \text{for } \nu = 1,\ldots,6 \\ 0, & \text{for } \nu = 0,7 \end{cases} \tag{9}$$

in which $u_{\rm dc} = U_{\rm dc}/\sqrt{2}U_{sN}$ and U_{sN} is the rms value of the phase voltage. By (9), $\mathbf{u}_\nu$ assumes six nonzero values (active vectors) and two zero values (zero vectors). It follows from (8) that

$$\boldsymbol{\psi}_s = \frac{1}{T_N}\int_0^t \mathbf{u}_\nu \, dt. \tag{10}$$

For six-step operation, the inverter output voltage constitutes a cyclic and symmetric sequence of active vectors, so that, in accordance with (10), the stator flux moves with constant speed along a hexagonal path [Fig. 3(c)]. The introduction of zero vectors stops the flux, an effect known as stop pulse, but does not change its path. There is only a change of cycle of the voltage vector sequence. This differs from sinusoidal PWM operation, where the inverter output voltage constitutes a suitable sequence

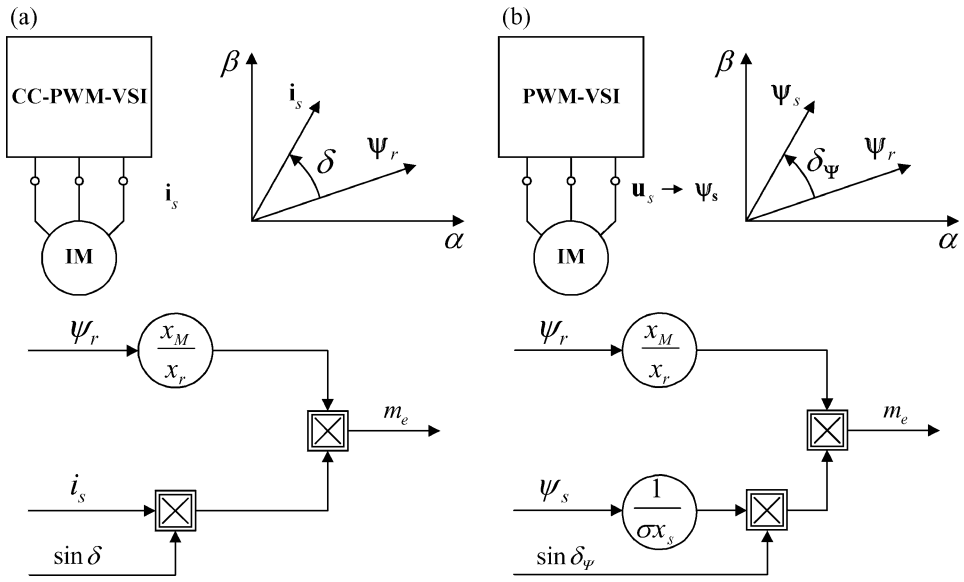

Fig. 2. Torque production. (a) FOC. (b) DTC.

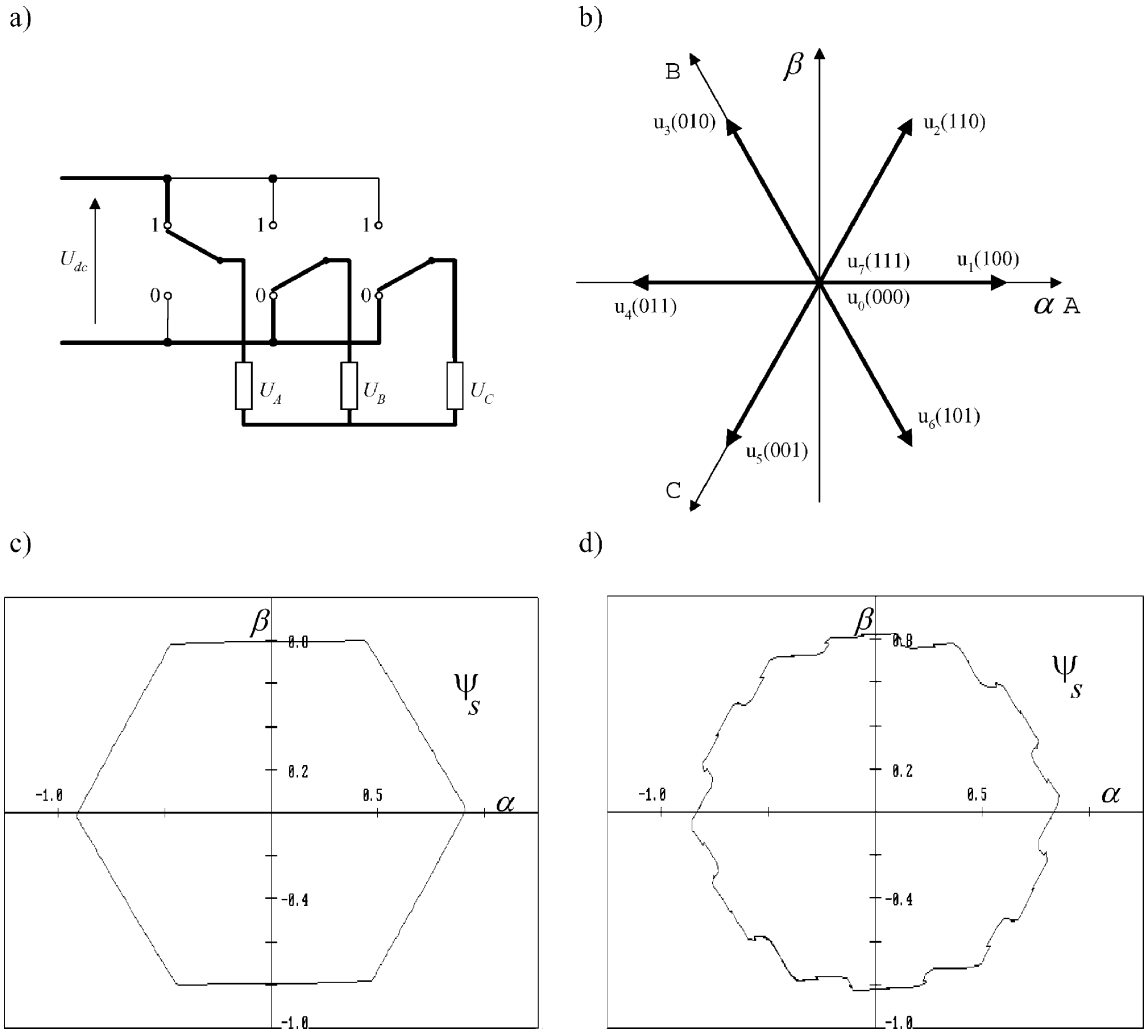

Fig. 3. (a) Simplified diagram of the VS inverter feeding an induction motor, (b) representation of output voltage vectors, (c) stator flux path in $\alpha-\beta$ plane under six-step operation, and (d) under sinusoidal PWM operation (low switching frequency).

of active and zero vectors and the stator flux moves along a track resembling a circle [Fig. 3(d)]. In any case, the rotor flux rotates continuously with the actual synchronous speed along a near-circular path, since it is smoothed by the rotor circuit fil-

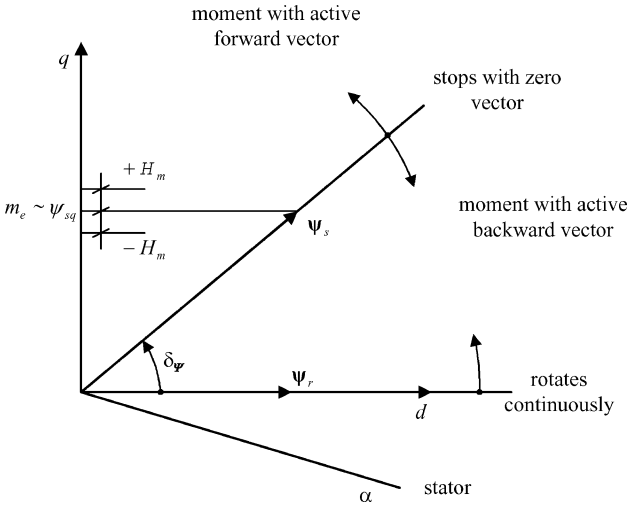

Fig. 4. Stator flux vector $\boldsymbol{\psi}_s$ movement relative to rotor flux vector $\boldsymbol{\psi}_r$ under the influence of active and zero voltage vectors.

tering action. Stator and rotor flux vectors are related by the following equation:

$$\boldsymbol{\psi}_s = \frac{l_M}{l_r}\boldsymbol{\psi}_r + \sigma l_s \mathbf{i}_s. \tag{11}$$

From the point of view of torque production it is the relative motion of the two vectors that is important, for they form the torque angle δ_ψ [Fig. 2(b)] that determines the instantaneous motor torque according to (7). Suppose that the rotor flux $\boldsymbol{\psi}_r$ moves slowly in the anticlockwise direction (Fig. 4). In such a case, forward switching of the active voltage vector causes a rapid movement of $\boldsymbol{\psi}_s$ away from $\boldsymbol{\psi}_r$ and, at the same time, a motor torque increase because of the raise of the torque angle δ_ψ. On the other hand when a zero vector is used, the stator flux $\boldsymbol{\psi}_s$ comes to a stop that, since $\boldsymbol{\psi}_r$ continues to move forward, causes a decrease in the torque angle δ_ψ and then in the motor torque m_e. If the duration T_0 of the zero state is sufficiently long, $\boldsymbol{\psi}_r$ will overtake $\boldsymbol{\psi}_s$; as a result, the angle δ_ψ and the motor torque will change direction. The important conclusion that follows from the above analysis is that there is a direct relationship between torque oscillations and the duration of zero states. By the cyclic switching of active and zero vectors, the motor torque is controlled. This is the principle of operation of the self-controlled modulator [19]. In the range of very low speeds ($< 0.2\omega_N$), the rotor flux $\boldsymbol{\psi}_r$ motion is too slow to achieve rapid torque reduction. In such a case, an active vector moving backward $\boldsymbol{\psi}_s$ is selected rather than a zero vector (Fig. 4). In the field-weakening region, zero vectors cannot be employed. Torque control is then achieved via a fast change of torque angle δ_ψ by advancing (to increase the torque) or retarding (to reduce it) the phase of the stator flux.

Summing up the outcomes so far obtained, the operation of a VS inverter-fed IM is characterized by the following properties.

- The inverter output voltage can only be in one of two states, either active (one of the nonzero vectors $\mathbf{u}_1, \ldots, \mathbf{u}_6$) or zero ($\mathbf{u}_0, \mathbf{u}_7$).
- The active forward vectors produce stator flux movement with constant linear speed while the zero vectors stop the flux; from the point of view of torque production, the two states correspond, respectively, to torque increase and torque reduction conditions.
- The active backward vectors produce stator field movement with constant linear speed in the opposite direction.
- For six-step operation (active vectors only), the stator flux moves along a hexagonal path with constant linear speed $\upsilon_s = (2/3)u_{\rm dc}T_N$ and an angular speed the average value of which is inversely proportional to the flux amplitude ($\omega_s = \upsilon_s\psi_s$).
- For sinusoidal PWM operation (active and zero vectors) and high switching frequency, the stator flux moves along a near-circular path with nearly constant angular speed equal to the actual synchronous speed.
- The rotor flux always moves continuously along a circular path with the actual synchronous angular speed.

B. Generic DTC Scheme

The generic DTC scheme for a VS-PWM inverter-fed IM drive is shown in Fig. 5(a). According to the previous discussion, the scheme includes two hysteresis controllers. The stator flux controller imposes the time duration of the active voltage vectors, which move the stator flux along the reference trajectory, and the torque controller determinates the time duration of the zero voltage vectors, which keep the motor torque in the defined-by-hysteresis tolerance band. At every sampling time the voltage vector selection block chooses the inverter switching state (S_A, S_B, S_C), which reduces the instantaneous flux and torque errors.

Compared to the conventional FOC scheme [Fig. 5(b)], the DTC scheme has the following features.

- There are no current control loops, hence, the current is not regulated directly.
- Coordinate transformation is not required.
- There is no separate voltage pulsewidth modulator.
- Stator flux vector and torque estimation is required.

Depending on how the switching sectors are selected, two different DTC schemes are possible. One, proposed by Takahashi and Noguchi [71], operates with circular stator flux vector path and the second one, proposed by Depenbrock, operates with hexagonal stator flux vector path [19]. The two switching sector selections are illustrated in Fig. 6(a) and (b), respectively.

III. Switching-Table-Based DTC (ST-DTC)

A. Basic ST-DTC Scheme

The block diagram of the ST-DTC scheme is shown in Fig. 7(a).

The command stator flux ψ_{sc} and torque m_c values are compared with the actual ψ_s and m_e values in hysteresis flux and torque controllers, respectively. The flux controller is a two-level comparator while the torque controller is a three-level comparator. The digitized output signals of the flux controller are defined as

$$d_\psi = 1 \quad \text{for} \quad \psi_s < \psi_{sc} - H_\psi \tag{12a}$$

$$d_\psi = 1 \quad \text{for} \quad \psi_s < \psi_{sc} + H_\psi \tag{12b}$$

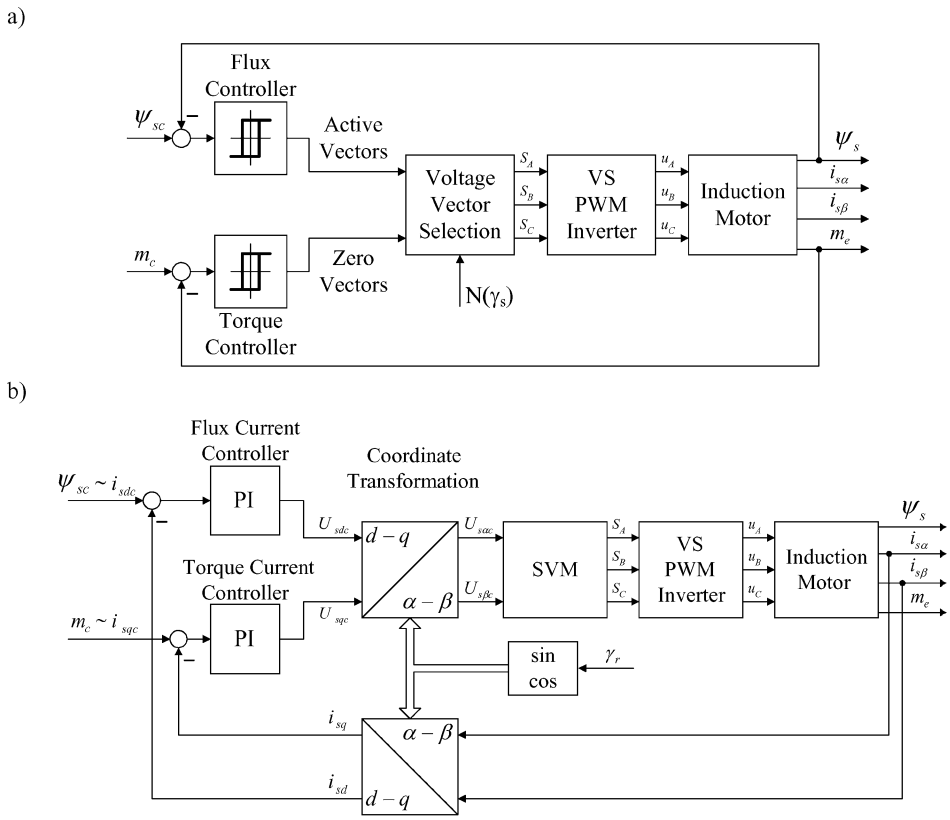

Fig. 5. Basic scheme of PWM inverter-fed induction motor with (a) DTC and (b) FOC.

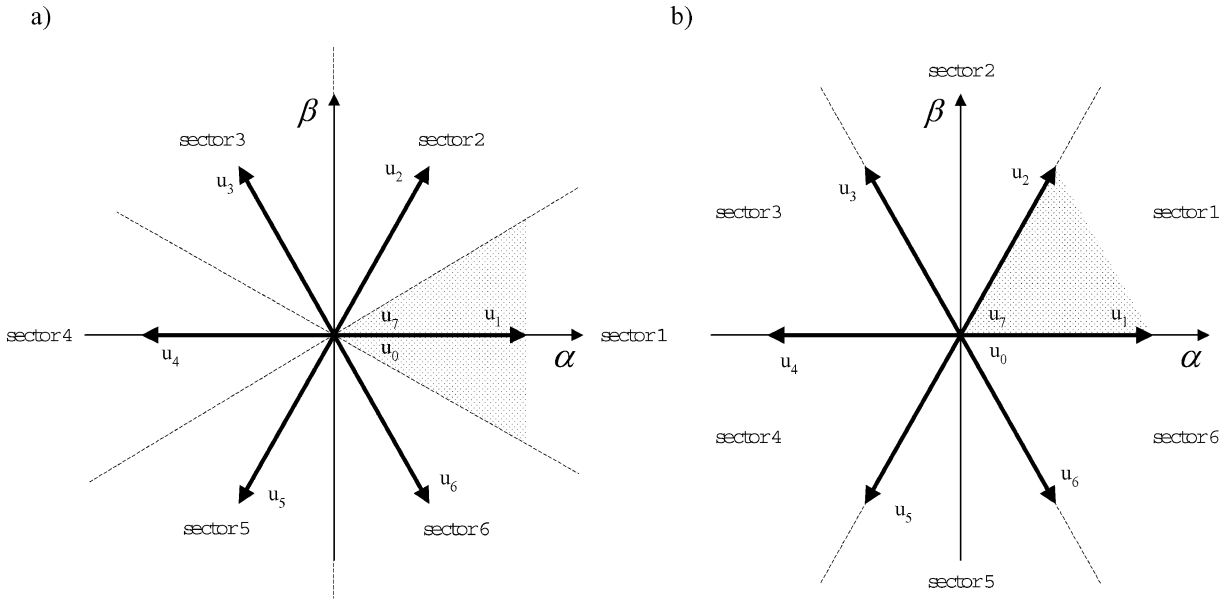

Fig. 6. Sector definition for (a) circular and (b) hexagonal stator flux vector path.

and those of the torque controller as

$$d_m = 1, \quad \text{for} \quad m_e < m_c - H_m \tag{13a}$$

$$d_m = 0, \quad \text{for} \quad m_e = m_c \tag{13b}$$

$$d_m = -1, \quad \text{for} \quad m_e < m_c + H_m \tag{13c}$$

where $2H_\psi$ is the flux tolerance band and $2H_m$ is the torque tolerance band.

The digitized variables d_ψ, d_m and the stator flux sector N, obtained from the angular position $\gamma_s = \operatorname{arctg}(\psi_{s\beta}/\psi_{s\alpha})$, create a digital word, which is used as the address for accessing an EPROM. By it, the appropriate voltage vector is selected according to Table I. The excellent dynamic performance of torque control is evident in Fig. 7(b), which shows torque reversal for half rated speed. Thanks to the selection of the appropriate backward voltage vector, torque reversal of rated

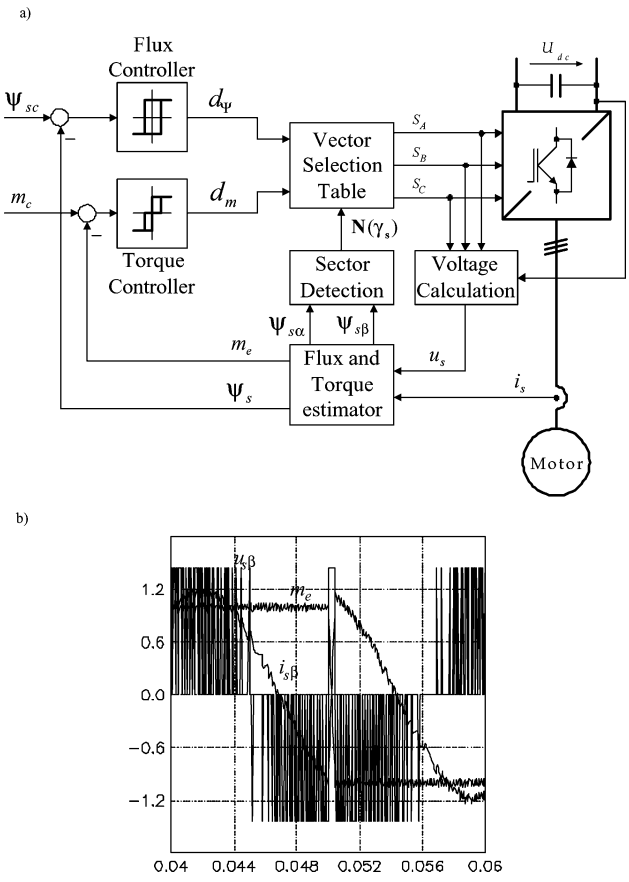

Fig. 7. ST-based DTC with circular stator flux path according to Takahashi and Noguchi. (a) Block scheme. (b) Typical transient response to rated torque reversal.

value takes place in about 1 ms, although it depends on the inverter supply voltage reserve. The characteristic features of the ST-DTC scheme of Fig. 7(a) include:

- nearly sinusoidal stator flux and current waveforms; the harmonic content is determined by the flux and torque controller hysteresis bands H_ψ and H_m;
- excellent torque dynamics;
- flux and torque hysteresis bands determine the inverter switching frequency, which varies with the synchronous speed and load conditions.

B. Modified ST-DTC

Many modifications of the basic ST-DTC scheme aimed at improving starting, overload conditions, very-low-speed operation, torque ripple reduction, variable switching frequency functioning, and noise level attenuation have been proposed during the last decade.

1) Improvement of Starting Conditions and Very-Low-Speed Performance: During starting and very-low-speed operation the basic ST-DTC scheme selects many times the zero voltage vectors resulting in flux level reduction owing to the stator resistance drop. This drawback can be avoided by using either a dither signal [38], [59] or a modified switching table in order to apply all the available voltage vectors in appropriate sequence [16], [79]. Also, predictive techniques can be used [2], [43].

2) Torque Ripple Reduction by Increased Number of Generated Inverter Switching States: Subdivision of the sampling period into two or three [14] equal time intervals leads to 12 or 56 voltage vectors, respectively (Fig. 8). The increased number of available voltage vectors allows both to subdivide the hysteresis of torque and flux controllers into more levels and to create a more accurate switching table that also takes into account the speed value.

3) Rotor Flux Amplitude Control: Under constant rotor flux operation the IM torque increases linearly with the slip frequency, and the maximum torque is limited only by the maximum current of the inverter. Therefore, in order to increase the torque overload capability of a ST-DTC scheme, the rotor flux instead of stator flux magnitude should be regulated. For given commands of rotor flux ψ_{rc} and torque m_c, the stator flux command needed by a ST-DTC scheme can be calculated as [14]

$$\psi_{sc} = \sqrt{\left(\frac{l_s}{l_M}\psi_{rc}\right)^2 + (\sigma l_s)^2 \left(\frac{l_r}{l_M}\frac{m_c}{\psi_{rc}}\right)^2}. \qquad (14)$$

However, the price for better overload capabilities is a higher parameter sensitivity of rotor flux magnitude control.

IV. Direct Self Control Scheme (DSC)

A. Basic DSC Scheme

The block diagram of the DSC scheme, proposed by Depenbrock [19], is shown in Fig. 9(a). Based on stator flux components $\psi_{s\beta A}$, $\psi_{s\beta B}$, and $\psi_{s\beta_C}$, the flux comparators generate the digitized variables d_A, d_B, and d_C, which correspond to active voltage vectors for six-step operation. The hysteresis torque controller, on the other hand, generates the digitized signal d_o that determines the zero states duration. Thus, in the constant flux region, the control algorithm is as follows:

$d_o = 1 \rightarrow S_A = d_B$, $S_B = d_C$, $S_C = d_A$, i.e., an active voltage vector is selected, defined by the flux comparators;
$d_o = 0 \rightarrow S_A = 0$, $S_B = 0$, $S_C = 0$, *or* $S_A = 1$, $S_B = 1$, $S_C = 1$, i.e., a zero voltage vector is selected.

In the field-weakening region, where the inverter is in six-step operation under rated output voltage, the torque is not determined by the hysteresis torque controller but by a momentary change of the stator flux amplitude $\Delta\psi_s$. In a simple case, it can be obtained by means of the PI-flux controller of Fig. 9(a). However, for precise control, more complex calculation is required [52], [69].

The dynamic performance of the torque control in the DSC scheme is shown in Fig. 9(b). In the basic version, DSC during torque reversal selects zero instead of a backward voltage vector [19]. The characteristic features of the DSC scheme of Fig. 9(a) are:

- PWM operation in the constant flux region and six-step operation in the field-weakening region;
- nonsinusoidal stator flux and current waveforms that, with the exception of the harmonics, are identical for both PWM and six-step operation;
- stator flux vector moves along a hexagon path also under PWM operation;

TABLE I
SELECTION OF VOLTAGE VECTORS IN THE BASIC ST-DTC

d_ψ d_m \ N(γ_s)		N=1	N=2	N=3	N=4	N=5	N=6
$d_\psi = 1$	$d_m = 1$	$\mathbf{u}_2(110)$	$\mathbf{u}_3(010)$	$\mathbf{u}_4(011)$	$\mathbf{u}_5(001)$	$\mathbf{u}_6(101)$	$\mathbf{u}_1(100)$
	$d_m = 0$	$\mathbf{u}_7(111)$	$\mathbf{u}_0(000)$	$\mathbf{u}_7(111)$	$\mathbf{u}_0(000)$	$\mathbf{u}_7(111)$	$\mathbf{u}_0(000)$
	$d_m = -1$	$\mathbf{u}_6(101)$	$\mathbf{u}_1(100)$	$\mathbf{u}_2(110)$	$\mathbf{u}_3(010)$	$\mathbf{u}_4(011)$	$\mathbf{u}_5(001)$
$d_\psi = 0$	$d_m = 1$	$\mathbf{u}_3(010)$	$\mathbf{u}_4(011)$	$\mathbf{u}_5(001)$	$\mathbf{u}_6(101)$	$\mathbf{u}_1(100)$	$\mathbf{u}_2(110)$
	$d_m = 0$	$\mathbf{u}_0(000)$	$\mathbf{u}_7(111)$	$\mathbf{u}_0(000)$	$\mathbf{u}_7(111)$	$\mathbf{u}_0(000)$	$\mathbf{u}_7(111)$
	$d_m = -1$	$\mathbf{u}_5(001)$	$\mathbf{u}_6(101)$	$\mathbf{u}_1(100)$	$\mathbf{u}_2(110)$	$\mathbf{u}_3(010)$	$\mathbf{u}_4(011)$

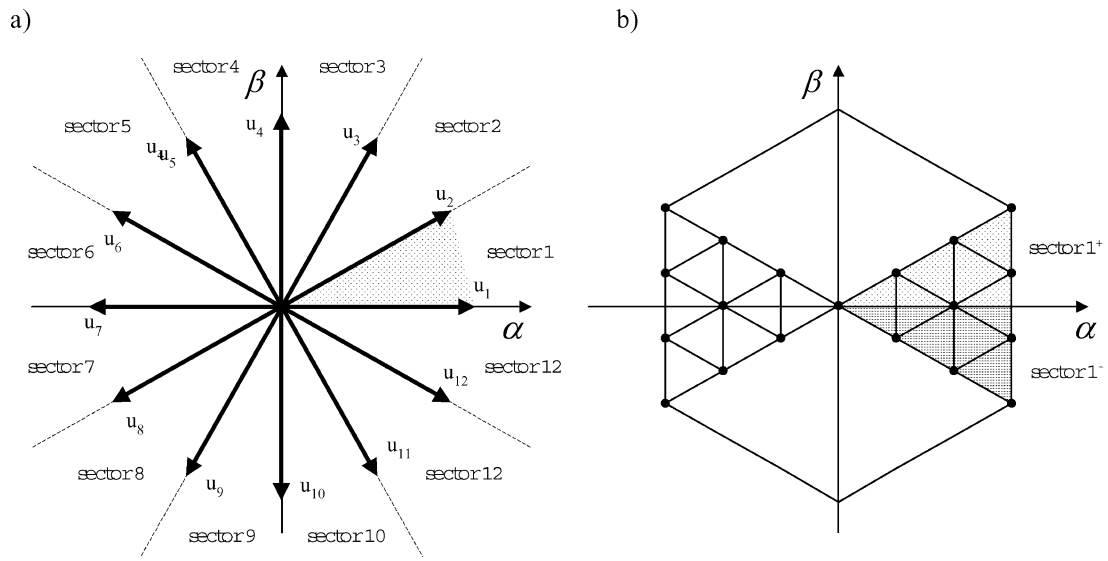

Fig. 8. Voltage vectors generated with (a) two and(b) three equal time intervals per cycle period.

- no voltage supply reserve is necessary and the inverter capability is fully utilized;
- the inverter switching frequency is lower than in the ST-DTC scheme of Fig. 7(a) because PWM is not of sinusoidal type as it turns out by comparing the voltage pattern in Figs. 7(b) and 9(b);
- excellent torque dynamics in constant and weakening field regions.

Note that the behavior of a DSC scheme can be reproduced by a ST-DTC scheme when the hysteresis band of the stator flux comparator is set at $H\psi = 0.076\ \psi_{sc}$ [11].

Low switching frequency and fast torque control even in the field-weakening region are the main reasons why the DSC scheme is convenient for high power traction drives [70], [80], [81].

B. Indirect Self Control (ISC)

In contrast to DTC—which, since the publication of [71], has been constantly developed and improved by many researchers and research centers—DSC has been studied and developed mainly by the Power Electronics Group of Ruhr University, Bochum, Germany, led by Depenbrock [29], [30], [33], [41], [52], [69]. To improve the DSC performance at the low-speed region, the method called ISC has been proposed [33]. In the first stage of development, this method was used in DSC drives only for starting and for operation up to 20%–30% of the rated speed [33]. Later, it was expanded as a new control strategy offered for inverters operated at high switching frequencies (>2 kHz) [30]. The ISC scheme, however, produces a circular stator flux path in association with a voltage pulsewidth modulator and, therefore, will be presented in the next section.

V. CONSTANT SWITCHING FREQUENCY DTC SCHEMES

A. Critical Evaluation of Hysteresis-Based DTC Schemes

The well-known disadvantages of the hysteresis-based DTC schemes are: variable switching frequency, violence of polarity consistency rules (to avoid ± 1 switching over dc-link voltage), current and torque distortion caused by sector changes, starting and low-speed operation problems, as well as high sampling frequency needed for digital implementation of hysteresis controllers.

When a hysteresis controller is implemented in a digital signal processor (DSP), its operation is quite different from that of the analog scheme. Fig. 10 illustrates a typical switching sequence in analog [Fig. 10(a)] and discrete [Fig. 10(b)] (also called sampled hysteresis) implementation. In analog implementation the torque ripple are kept exactly within the hysteresis band and the switching instants are not equally

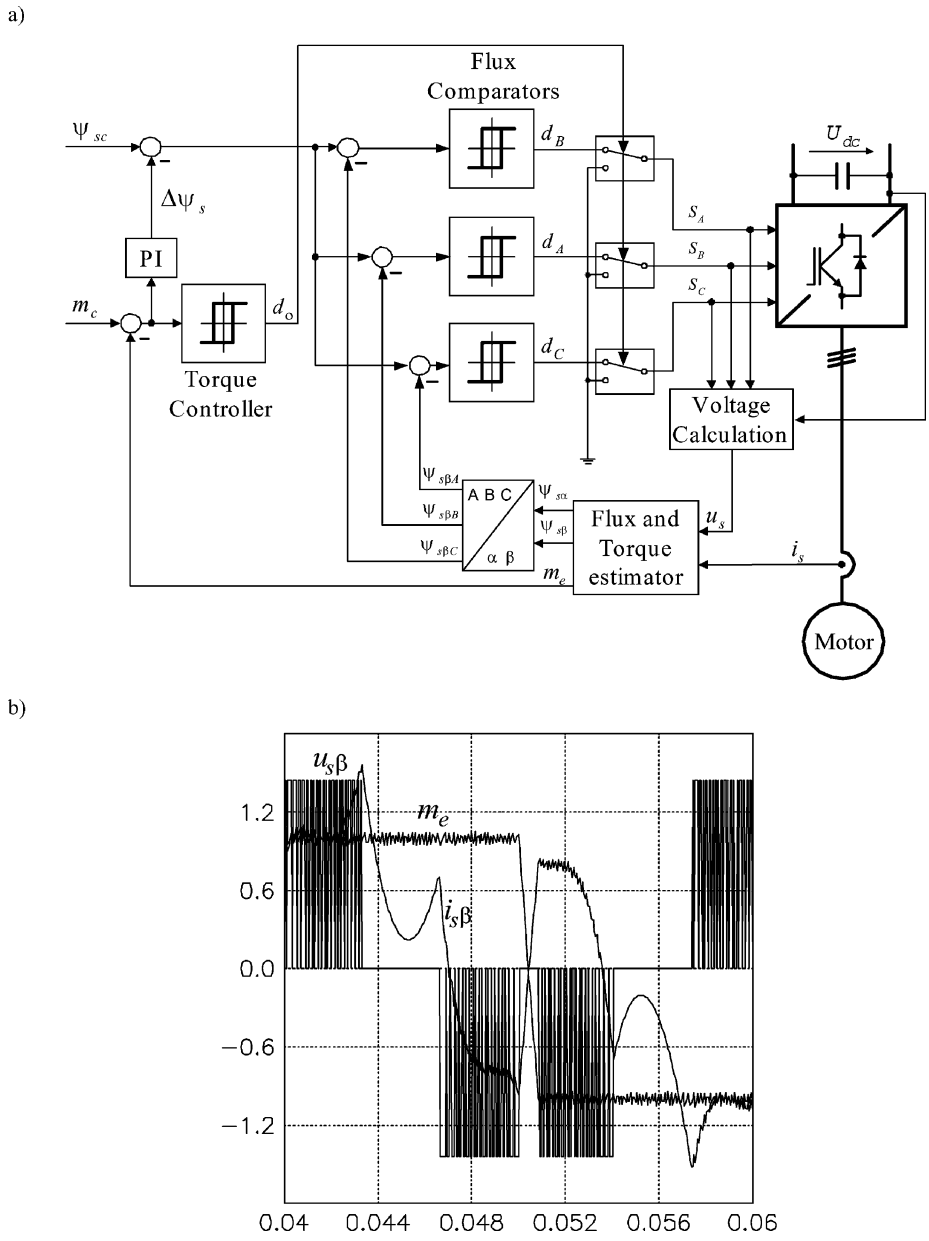

Fig. 9. DSC with hexagonal stator flux path according to Depenbroeck. (a) Block scheme. (b) Typical transient response to rated torque reversal.

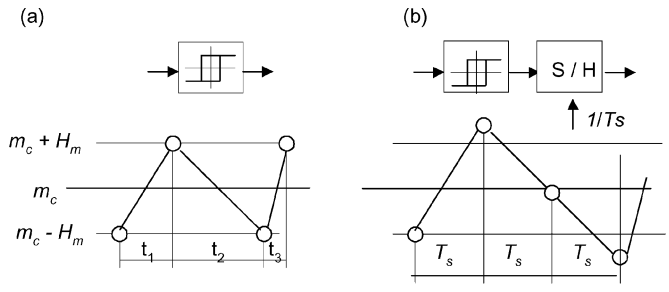

Fig. 10. Operation of the (a) analog and (b) discrete hysteresis controller.

spaced. In contrast, the discrete system operates at fixed sampling time T_s and if

$$2H_m \gg \frac{dm_{\max}}{dt} \cdot T_s \tag{15}$$

the discrete controller will operate like the analog one. However, it requires fast sampling. All the above difficulties can be eliminated when, instead of the switching table, a voltage pulsewidth modulator is used.

Basically, the DTC strategies operating at constant switching frequency can be implemented by means of closed-loop schemes with PI, predictive/dead-beat or neuro-fuzzy (NF) controllers. The controllers calculate the required stator voltage vector, averaged over a sampling period. The voltage vector is finally synthesized by a PWM technique, which in most cases is the space-vector modulation (SVM). Therefore, differently from the conventional DTC solution, in a DTC-SVM scheme the switching harmonics are neglected in the control algorithm.

B. DTC-SVM Scheme With Closed-Loop Flux Control

In the DTC-SVM scheme of Fig. 11(a), the stator flux components in the rotor flux coordinates ψ_{sdc}, ψ_{sqc} are calculated

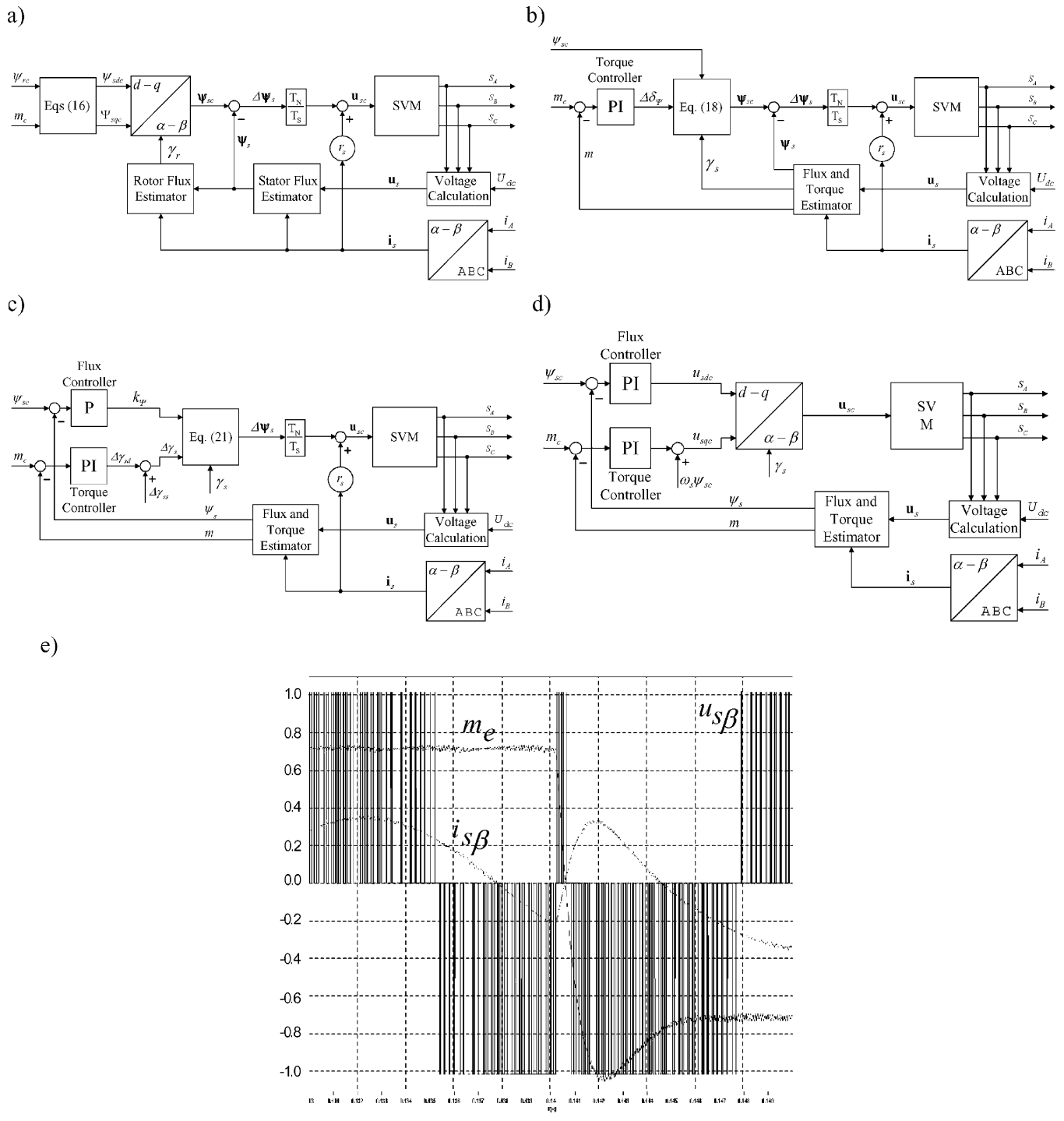

Fig. 11. Basic variants of DTC-SVM schemes. (a) DTC-SVM with closed flux control [15]. (b) DTC-SVM with closed-loop torque control [84], [85]. (c) DTC-SVM scheme operated in polar coordinates—ISC [30], [32]. (d) DTC-SVM scheme operated in Cartesian coordinates—stator-flux-oriented control [1], [88]. (e) Transient response to rated torque reversal of the DTC-SVM scheme from Fig. 11(d).

from the commanded values of torque m_c and rotor flux magnitude ψ_{rc} according to the following equations:

$$\psi_{sdc} = \frac{l_s}{l_M}\left(1 + \sigma T_r \frac{d\psi_{rc}}{dt}\right) \tag{16a}$$

$$\psi_{sqc} = \frac{l_s}{l_M}\sigma l_s \frac{m_c}{\psi_{rc}} \tag{16b}$$

where T_r is the rotor time constant. The command value of the stator flux vector $\boldsymbol{\psi}_{sc}$, after coordinate transformation $dq/\alpha\beta$, is compared with the estimated value $\boldsymbol{\psi}_s$ and the error together with the stator resistance drop, allows for the calculation of the appropriate stator voltage vector $\mathbf{u}_{sc}$ which is applied to the IM in the next sampling period

$$\mathbf{u}_{sc} = \frac{T_N}{T_s}\Delta\boldsymbol{\psi}_s + r_s \cdot \mathbf{i}_s. \tag{17}$$

As mentioned in Section III-B.3, the use of rotor instead of stator flux magnitude improves the torque overload capabilities of IM.

C. DTC-SVM Scheme With Closed-Loop Torque Control

The DTC-SVM scheme of Fig. 11(a) requires stator and rotor flux vector estimators and, therefore, all IM parameters have to be known. To enhance the dynamic and steady-state performance of the torque response a variant of the scheme with closed-loop torque control can be used [Fig. 11(b)] [84], [85]. In this scheme the torque controller generates the command value of the torque angle increment $\Delta\delta\psi$, which is added to the stator flux position γ_s in the stator reference frame α, β to calculate the stator flux vector command $\boldsymbol{\psi}_{SC}$ according to

$$\boldsymbol{\psi}_{sc} = \boldsymbol{\psi}_{sc} e^{j(\gamma_s + \Delta\delta_\Psi)}. \tag{18}$$

The commanded stator flux vector $\boldsymbol{\psi}_{sc}$ is compared with the estimated one $\boldsymbol{\psi}_s$ and the resultant error $\Delta\boldsymbol{\psi}_{\mathbf{s}}$ is used for calculation of the commanded stator voltage vector according to (17).

D. DTC-SVM Scheme With Closed-Loop Torque and Flux Control Operating in Polar Coordinates—ISC

Further improvement can be achieved when both torque and stator flux magnitude are controlled in a closed-loop way. The version operating in polar coordinates is shown in Fig. 11(c) [29], [30]. In this scheme the error of the stator flux vector $\Delta\boldsymbol{\psi}_{\mathbf{s}}$ is calculated from the outputs k_ψ and $\Delta\gamma_s$ of the flux and torque controllers as follows:

$$\begin{aligned}\Delta\boldsymbol{\psi}_s(k) &= \boldsymbol{\psi}_s(k) - \boldsymbol{\psi}_s(k-1) \\ &= \left\{[1 + k_\psi(k)] \cdot e^{j\Delta\gamma_s(k)} - 1\right\} \cdot \boldsymbol{\psi}_s(k-1).\end{aligned} \tag{19}$$

With the approximation

$$e^{j\Delta\gamma_s(k)} \cong 1 + j\Delta\gamma_s(k). \tag{20}$$

Equation (19) can be written in the form

$$\Delta\boldsymbol{\psi}_s = [k_\psi(k) + j\Delta\gamma_s(k)] \cdot \boldsymbol{\psi}_s(k-1). \tag{21}$$

The last equation is used to calculate the commanded stator voltage vector according to (17). To improve the dynamic performance of the torque control, the angle increment $\Delta\gamma_s$ is composed of two parts: the dynamic part $\Delta\gamma_{sd}$ delivered by the torque controller and the stationary part $\Delta\gamma_{ss}$ generated by a feedforward loop.

E. DTC-SVM Scheme With Closed-Loop Torque and Flux Control Operating in Cartesian Coordinates—Stator-Flux-Oriented Control

The outputs of the PI flux and torque controllers can be interpreted as the d–q stator voltage components u_{sdc}, u_{sqc} in the stator flux oriented coordinates giving the block scheme of Fig. 11(d) [1], [88]. The control strategy relies on a simplified description of the stator voltage components, expressed in stator-flux-oriented coordinates as

$$u_{sd} = r_s \cdot i_{sd} + \frac{d\psi_{sc}}{dt} \approx \frac{d\psi_{sc}}{dt} \tag{22a}$$

$$u_{sq} = r_s \cdot i_{sq} + \omega_s\psi_{sc} = k_s m_c + \omega_s\psi_{sc} \tag{22b}$$

where $k_s = r_s/\psi_{sc}$ and ω_s is the angular speed of the stator flux vector. The above equations show that the component u_{sd} has influence only on the change of stator flux magnitude, and the component u_{sq}—if the term $\omega_s\psi_s$ is decoupled—can be used for torque adjustment. Therefore, after coordinate transformation $dq/\alpha\beta$ into the stationary frame, the command values $u_{s\alpha c}$, $u_{s\beta c}$ are delivered to SVM.

Note that calculation of the commanded stator voltage vector by (22) requires the derivative of the stator flux magnitude, which is a dc quantity. Then, the scheme of Fig. 11(d) is less noisy than the previously presented schemes of Fig. 11(a)–(c) that are based on (17). Also, hybrid DTC/DTC-SVM solutions have been proposed [40], [46], where the conventional ST-DTC scheme operates only in dynamic states.

F. Dead-Beat DTC-SVM Schemes

The main idea behind a dead-beat DTC scheme is to force torque and stator flux magnitude to achieve their reference values in one sampling period by synthesizing a suitable stator voltage vector applied by SVM.

In the approach proposed by Habetler *et al.* [25], [26], the changes of torque and flux over one sampling period are at first predicted from the motor equations, and then a quadratic equation is solved to obtain the command value of stator voltage vector in stationary coordinates. This time-consuming algorithm is used in steady state. During transients, an alternative algorithm is adopted and the appropriate voltage vector is selected *a priori* from a switching table, which includes only active vectors. Such a solution guarantees fast elimination of transient errors.

Due to the limitation of inverter voltages and currents, dead-beat control is not always possible. Based on a discrete model of an IM, Maes and Melkebeek [51] have proposed an algorithm, called direct time DTC, which uses a prediction of the back electromotive force (EMF). The DTC algorithm also incorporates the limitation of the inverter voltage and current as well as compensation of the calculation delay.

Lee *et al.* [47] have developed another interesting approach based on a dead-beat digital controller instead of a PI controller for the DTC-SVM scheme of Fig. 11(d). In the paper the z-domain design of the transfer function $G_R(z)$ of the flux and torque controllers is carried out starting from the desired closed-loop transfer function $F(z)$

$$G_R(z) = \frac{F(z)}{G_s(z)[1 - F(z)]} \tag{23}$$

where $G_s(z)$ is the open-loop transfer function. The DTC-SVM scheme of Fig. 11(d) with torque and flux controllers implemented by this method exhibits good steady-state and dynamic performance, even for low switching frequency (0.5–2 kHz). Therefore, it can be used in high-performance high-power drives (traction applications).

G. NF DTC-SVM Scheme

In the last decade a fast development of artificial-intelligence-based controllers has been observed. They have expanded also

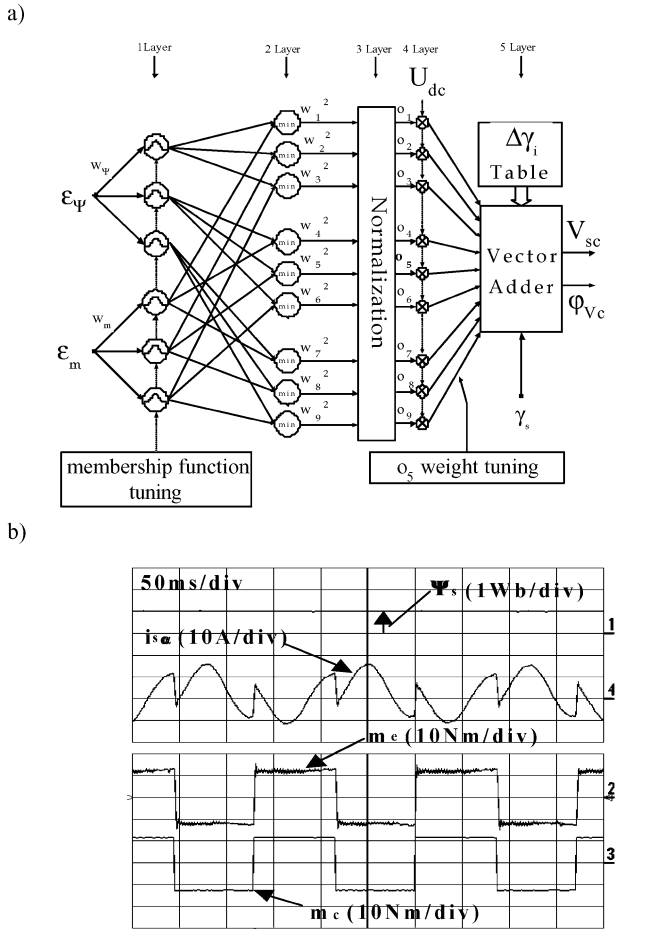

Fig. 12. NF DTC-SVM. (a) Block scheme. (b) Experimental oscillograms illustrating torque-tracking performance.

in the area of power electronics and drive control [10], [37], [40], [78]. The combination of fuzzy logic and artificial neural networks has been proved to be powerful as it offers all the advantages of both techniques. The initial structure of the controllers is commonly built up using the human expert knowledge [3], [36], [54]–[56], [78], [83].

A controller based on *Adaptive NF Inference System* (ANFIS) for voltage space-vector generation has been proposed by Grabowski *et al.* [23]. It combines fuzzy logic and artificial neural networks for decoupled flux and torque control. In the scheme, shown in Fig. 12(a), the error signals ε_ψ and ε_m are delivered to the NF controller, which is also entered by the actual position (γ_s) of the stator flux vector. The NF controller determinates the stator voltage command vector in polar coordinates $\mathbf{v}_c = [V_{sc}, \varphi_{Vc}]$ for the SVM block. The scheme is characterized by a simple self-tuning procedure and good steady-state and dynamic performance [Fig. 12(b)].

VI. Direct Torque Control of Synchronous Motors

DTC adjusts motor torque and stator flux magnitude in a closed-loop fashion where the feedback values are estimated from stator voltage and current vectors in stator-fixed coordinates. Therefore, it is a general control strategy independent of rotor parameters and can be applied not only to an IM but also to all types of synchronous motors: permanent-magnet synchronous motors (PMSMs), field winding excited synchronous motors (FESMs), reluctance synchronous motors (RSMs), and switched reluctance motors (SRMs) [8], [40], [68], [79], [91]. In all cases both hysteresis-based DTC [63]–[67], [72], [89] and DTC-SVM [84]–[87] schemes can be used.

A. DTC of PMSM

In contrast to IMs, the initial value of the stator flux in PMSMs is not zero and depends on the rotor position. In motion- sensorless PMSM drives the initial position of the rotor is unknown and this often causes initial backward rotation and problems of synchronization. For nonsalient (with surface-mounted magnets) PMSMs, reliable position estimation is more difficult than for salient (with buried or inserted magnets) construction [27], [64], [65], [67], [72], [75], where the initial position can be calculated univocally by exploiting the sinusoidal inductance variation. For a nonsalient PMSM to start with light loads, a simple low-pass filter instead of a pure integrator in the flux estimator can be used [91], [92]. This solves the problem of flux initial conditions. Another method used to estimate the initial position of the rotor is the motor supply by a fixed active voltage vector while limiting current by applying zero vectors.

B. DTC of FESM

In FESMs the initial rotor position can be estimated using induced stator current variation [8], [10], [22]. During magnetizing operation the stator flux is estimated from the induced stator current. Once the stator flux reaches a minimum value, torque reference is applied. The exciting current can be regulated in sensorless fashion by extending the classical DTC or DTC-SVM scheme with a reactive torque closed-loop control [91].

C. DTC of RSM

RSMs are characterized by special rotor configurations, which are constructed with the aim to realize high L_d/L_q ratio, in the range 2–10, to guarantee high reluctance torque. With $L_d/L_q = 8 \ldots 10$, RSMs are fully competitive with IMs in terms of torque density, power factor, and efficiency; in addition, the absence of rotor currents makes control of RSMs simpler than IMs. As in IMs, the initial flux is zero [8], [10], [40]. The DTC scheme for an RSM is quite similar to that presented in Fig. 8 for an IM. In order to reduce torque and current pulsations, the DTC-SVM scheme or hybrid DTC/DTC-SVM variants have also been proposed for an RSM [40], [46]. To avoid high startup currents, an initial magnetization is necessary [91].

D. DTC of SRM

The main motivation in usage of an SRM is its simple and robust mechanical structure, which is associated with high torque density. However, an SRM does not have a sinusoidal arrangement for the windings, but a concentrated one. The double-salient structure together with the concentrated winding arrangement leads to severe torque pulsations and, as a consequence, to noise trouble. The most popular methods of torque-ripple reduction are based on current-profiling techniques with a fast current control loop. However, if the instantaneous torque of an SRM is estimated by help of the machine characteristics, the DTC scheme without current control loop can be implemented [16], [32]. A multi-hysteresis-based DTC scheme

such as that described in [32] is able to compensate for the inherent torque ripple during phase commutation and to perform maximum torque response and control robustness.

VII. Conclusion

This paper has reviewed DTC strategies for PWM inverter-fed ac motor drives. DTC represents a viable alternative to FOC, being also a general philosophy for controlling the ac drives in both motor and generator mode of operation. From a general perspective, FOC requires an accurate estimation of the rotor flux vector. However, when an accurate estimation of the motor flux is available, there is no need to set up a current control loop and DTC is the natural solution.

The main features of DTC can be summarized as follows.

- DTC operates with closed torque and flux loops but without current controllers.
- DTC needs stator flux and torque estimation and, therefore, is not sensitive to rotor parameters.
- DTC is inherently a motion-sensorless control method.
- DTC has a simple and robust control structure; however, the performance of DTC strongly depends on the quality of the estimation of the actual stator flux and torque.

Starting from the IM drives, the DTC strategies have been divided into three groups: hysteresis-based ST DTC, hysteresis-based DSC, and constant-switching-frequency DTC schemes operating in association with space-vector modulators (DTC-SVM). The basic principles and the latest progress of these strategies have been systematically presented. Their advantages and limitations have been briefly examined and the application fields have been indicated.

DSC is preferred for high-power low-switching-frequency drives and is very effective in the square-wave operation region where fast flux weakening and torque control are achieved. Therefore, it is well suited for traction and vehicle drives.

Constant-switching-frequency DTC-SVM schemes improve considerably the drive performance in terms of reduced torque and flux pulsations, reliable startup and low-speed operation, well-defined harmonic spectrum, and radiated noise. Therefore, DTC-SVM is an excellent solution for general-purpose IM and PMSM drives in a very wide power range. Instead, the short sampling time required by the ST-DTC schemes makes them suited to very fast torque- and flux-controlled drives because of the simplicity of the control algorithm. As a conclusion of the survey, it is the belief of the authors that the DTC strategy will continue to play a strategic role in the development of high-performance motion-sensorless ac drives.

References

[1] U. Baader, "High dynamic torque control of induction motor in stator flux oriented coordinates" (in German), *ETZ Arch.*, vol. 11, no. 1, pp. 11–17, 1998.

[2] U. Baader, M. Depenbrock, and G. Gierse, "Direct self control (DSC) of inverter-fed-induction machine—A basis for speed control without speed measurement," *IEEE Trans. Ind. Applicat.*, vol. 28, pp. 581–588, May/June 1992.

[3] M. Bertoluzzo, G. Buja, and R. Menis, "Analytical formulation of the direct control of induction motor drives," in *Proc. IEEE Int. Symp. Industrial Electronics*, 1999, pp. 14–20.

[4] ——, "Operation of DFTC IM drives under estimation process errors," in *Proc. Int. Conf. Power Electronics and Motion Control*, 2000, pp. 1.27–1.34.

[5] F. Blaschke, "The principle of field-orientation as applied to the transvector closed-loop control system for rotating-field machines," *Siemens Rev.*, vol. 34, pp. 217–220, 1972.

[6] M. Bodson, J. Chiasson, and R. Novotnak, "High performance induction motor control via input-output linearization," *IEEE Contr. Syst. Mag.*, vol. 14, pp. 25–33, Aug. 1994.

[7] I. Boldea and S. A. Nasar, "Torque vector control. A class of fast and robust torque, speed and position digital controllers for electric drives," *Electromech. Power Syst.*, vol. 15, pp. 135–147, 1988.

[8] ——, *Electric Drives*. Boca Raton, FL: CRC Press, 1999.

[9] F. Bonanno, A. Consoli, A. Raciti, and A. Testa, "An innovative direct self-control scheme for induction motor drives," *IEEE Trans. Power Electron.*, vol. 12, pp. 800–806, Sept. 1997.

[10] B. K. Bose, *Modern Power Electronics and AC Drives*. Englewood Cliffs, NJ: Prentice-Hall, 2001.

[11] G. Buja, D. Casadei, and G. Serra, "DTC-Based strategies for induction motor drives," in *Proc. IEEE IECON'97*, vol. 4, 1997, pp. 1506–1516.

[12] G. Buja, "A new control strategy of the induction motor drives: The direct flux and torque control," *IEEE Ind. Electron. Newslett.*, vol. 45, pp. 14–16, Dec. 1998.

[13] L. A. Cabrera, M. E. Elbuluk, and D. S. Zinger, "Learning techniques to train neural networks as a state selector for inverter-fed induction machines using direct torque control," *IEEE Trans. Power Electron.*, vol. 12, pp. 788–799, Sept. 1997.

[14] D. Casadei, F. Profumo, G. Serra, and A. Tani, "FOC and DTC: Two viable schemes for induction motors torque control," *IEEE Trans. Power Electron.*, vol. 17, pp. 779–787, Sept. 2002.

[15] D. Casadei, G. Serra, and A. Tani, "Constant frequency operation of a DTC induction motor drive for electric vehicle," in *Proc. ICEM'96*, vol. 3, 1996, pp. 224–229.

[16] A. D. Cheok and P. H. Hoon, "A new torque control method for switched reluctance motor drives," in *Proc. IEEE IECON'00*, 2000, CD-ROM.

[17] V. Cascone, L. Mantica, and M. Oberti, "Three level inverter DSC control strategy for traction drives," in *Proc. 5th Eur. Conf. Power Electronics and Applications*, vol. 1, Florence, Italy, 1989, pp. 135–139.

[18] S. Chung, H.-S. Kim, C.-G. Kim, and M.-J. Youn, "A new instantaneous torque control of PM synchronous motor for high-performance direct-drive applications," *IEEE Trans. Power Electron.*, vol. 13, pp. 388–400, May 1998.

[19] M. Depenbrock, "Direct self control of inverter-fed induction machines," *IEEE Trans. Power Electron.*, vol. 3, pp. 420–429, Oct. 1988.

[20] ——, "Direct self-control of the flux and rotary moment of a rotary-field machine," U.S. Patent 4 678 248, July 7, 1987.

[21] "Direct torque control—The world's most advanced AC drive technology," ABB Finland, Helsinki, Tech. Guide 1, 1996.

[22] C. French and P. Acarnley, "Direct torque control of permanent magnet drives," *IEEE Trans. Ind. Applicat.*, vol. 32, pp. 1080–1088, Sept./Oct. 1996.

[23] P. Z. Grabowski, M. P. Kazmierkowski, B. K. Bose, and F. Blaabjerg, "A simple direct-torque neuro-fuzzy control of PWM-inverter-fed induction motor drive," *IEEE Trans. Ind. Electron.*, vol. 47, pp. 863–870, Aug. 2000.

[24] T. G. Habetler and D. D. Divan, "Control strategies for direct torque control using discrete pulse modulation," *IEEE Trans. Ind. Applicat.*, vol. 27, pp. 893–901, Sept./Oct. 1991.

[25] T. G. Habetler, F. Profumo, and M. Pastorelli, "Direct torque control of induction machines over a wide speed range," in *Conf. Rec. IEEE-IAS Annu. Meeting*, 1992, pp. 600–606.

[26] T. G. Habetler, F. Profumo, M. Pastorelli, and L. M. Tolbert, "Direct torque control of induction motor using space vector modulation," *IEEE Trans. Ind. Applicat.*, vol. 28, pp. 1045–1053, Sept./Oct. 1992.

[27] M. E. Haque, L. Zhong, and M. F. Rahman, "A sensorless speed estimation for application in a direct torque controller of an interior permanent magnet synchronous motor drive, incorporating compensation of offset error," in *Proc. IEEE PESC'02*, vol. 1, 2002, pp. 276–281.

[28] K. Hasse, "Drehzahlgelverfahren für schnelle umkehrantriebe mit stromrichtergespeisten asynchron-kurzschlusslaufer-motoren," *Reglungstechnik*, vol. 20, pp. 60–66, 1972.

[29] F. Hoffman, "Drehgeberlose Geregelte Induktionsmaschinen an IGBT-Pulsstromrichtern," Ph.D. thesis, Ruhr-Univ. Bochum, Bochum, Germany, 1996.

[30] F. Hoffman and M. Janecke, "Fast torque control of an IGBT-inverter-fed tree-phase A.C. drive in the whole speed range—Experimental result," in *Proc. EPE Conf.*, 1995, pp. 3.399–3.404.

[31] N. R. N. Idris and A. H. Yatim, "Reduced torque ripple and constant torque switching frequency strategy for induction motors," in *Proc. IEEE APEC'00*, 2000, pp. 154–161.

[32] R. B. Inderka and R. W. De Doncker, "DITC—Direct instantaneous torque control of switched reluctance drives," *IEEE Trans. Ind. Applicat.*, vol. 39, pp. 1046–1051, July/Aug. 2003.

[33] M. Janecke, R. Kremer, and G. Steuerwald, "Direct self-control, a novel method of controlling asynchronous machines in traction applications," in *Proc. EPE Conf.*, vol. 1, Aachen, Germany, 1989, pp. 75–81.

[34] R. Jönsson, "Method and apparatus for controlling an AC induction motor," U.S. Patent 5 294 876, Mar. 15, 1994.

[35] R. Jönsson and W. Leonhard, "Control of an induction motor without a mechanical sensor, based on the principle of "natural field orientation" (NFO)," in *Proc. IPEC Conf.*, Yokohama, Japan, 1995, pp. 298–303.

[36] M. P. Kazmierkowski and H. Tunia, *Automatic Control of Converter Fed Drives*. Amsterdam, The Netherlands: Elsevier, 1994.

[37] M. P. Kazmierkowski and T. Orlowska-Kowalska, "ANN based estimation and control in converter-fed induction motor drives," in *Soft Computing in Industrial Electronics*, S.J. Ovaska and L. Sztandera, Eds. Heidelberg, Germany: Physica Verlag, 2002, pp. 45–94.

[38] M. P. Kazmierkowski and A. Kasprowicz, "Improved direct torque and flux vector control of PWM inverter-fed induction motor drives," *IEEE Trans. Ind. Electron.*, vol. 42, pp. 344–350, Aug. 1995.

[39] M. P. Kazmierkowski and D. L. Sobczuk, "Sliding mode feedback linearized control of PWM inverter-fed induction motor," in *Proc. IEEE IECON'96*, Taipei, Taiwan, R.O.C., 1996, pp. 244–249.

[40] M. P. Kazmierkowski, R. Krishnan, and F. Blaabjerg, Eds., *Control in Power Electronics*. San Diego, CA: Academic, 2002.

[41] S. Koch, "Beiträge zur Regelung von Induktionsmaschinen ohne Drehgeber," Ph.D. thesis, Ruhr-Univ. Bochum, Bochum, Germany, 1998.

[42] J. K. Kang and S. K. Sul, "New direct torque control of induction motor for minimum torque ripple and constant switching frequency," *IEEE Trans. Ind. Applicat.*, vol. 35, pp. 1076–1082, Sept./Oct. 1999.

[43] ——, "Analysis and prediction of inverter switching frequency in direct torque control of induction machine based on hysteresis bands and machine parameters," *IEEE Trans. Ind. Electron.*, vol. 48, pp. 545–553, June 2001.

[44] R. Krishnan, *Electric Motor Drives*. Englewood Cliffs, NJ: Prentice-Hall, 2001.

[45] Z. Krzeminski, "Nonlinear control of induction motors," in *Proc. 10th IFAC World Congr.*, Munich, Germany, 1987, pp. 349–354.

[46] C. Lascu, I. Boldea, and F. Blaabjerg, "A modified direct torque control (DTC) for induction motor sensorless drive," in *Conf. Rec. IEEE-IAS Annu. Meeting*, 1998, pp. 415–422.

[47] J. H. Lee, C. G. Kim, and M. J. Youn, "A dead-beat type digital controller for the direct torque control of an induction motor," *IEEE Trans. Power Electron.*, vol. 17, pp. 739–746, Sept. 2002.

[48] B. S. Lee and R. Krishnan, "Adaptive stator resistance compensation for high performance direct torque controlled induction motor drives," in *Conf. Rec. IEEE-IAS Annu. Meeting*, vol. 1, 1998, pp. 423–430.

[49] C. Lochot, X. Roboam, and P. Maussion, "A new direct torque control strategy for an induction motor with constant switching frequency operation," in *Proc. EPE Conf.*, vol. 2, 1995, pp. 431–436.

[50] J. N. Nash, "Direct torque control, induction motor vector control without an encoder," *IEEE Trans. Ind. Applicat.*, vol. 33, pp. 333–341, Mar./Apr. 1997.

[51] J. Maes and J. Melkebeek, "Discrete direct torque control of induction motors using back e.m.f. measurements," in *Conf. Rec. IEEE-IAS Annu. Meeting*, vol. 1, 1998, pp. 407–414.

[52] D. Maischak, "Schnelle Drehmomentregelung im Gesamten Drehzahlbereich Eines Hochausgenutzten Drehfeldantriebes," Ph.D. thesis, Ruhr-Univ. Bochum, Bochum, Germany, 1994.

[53] R. Marino, "Output feedback control of current-fed induction motors with unknown rotor resistance," *IEEE Trans. Contr. Syst. Technol.*, vol. 4, pp. 336–347, July 1996.

[54] S. A. Mir, D. S. Zinger, and M. E. Elbuluk, "Fuzzy controller for inverter fed induction machines," *IEEE Trans. Ind. Applicat.*, vol. 30, pp. 78–84, Jan./Feb. 1994.

[55] S. Mir, M. E. Elbuluk, and D. S. Zinger, "PI and fuzzy estimators for the stator resistance in direct torque control of induction motors," in *Proc. IEEE PESC'94*, 1994, pp. 744–751.

[56] S. A. Mir and M. E. Elbuluk, "Precision torque control in inverter-fed induction machines using fuzzy logic," in *Proc. IEEE PESC'95*, 1995, pp. 396–401.

[57] N. Mohan, *Advanced Electric Drives*. Minneapolis, MN: MNPERE, 2001.

[58] P. Mutschler and E. Flach, "Digital implementation of predictive direct control algorithms for induction motors," in *Conf. Rec. IEEE-IAS Annu. Meeting*, 1998, pp. 444–451.

[59] T. Noguchi, M. Yamamoto, S. Kondo, and I. Takahashi, "High frequency switching operation of PWM inverter for direct torque control of induction motor," in *Conf. Rec. IEEE-IAS Annu. Meeting*, 1997, pp. 775–780.

[60] R. Ortega, A. Loria, P. J. Nicklasson, and H. Sira-Ramirez, *Passivity-Based Control of Euler-Lagrange Systems*. London, U.K.: Springer-Verlag, 1998.

[61] M. Pietrzak-David and B. de Fornel, "Non-Linear control with adaptive observer for sensorless induction motor speed drives," *EPE J.*, vol. 11, no. 4, pp. 7–13, 2001.

[62] P. Pohjalainen and C. Stulz, "Method and apparatus for direct torque control of a three-phase machine," U.S. Patent 5 734 249, Mar. 31, 1998.

[63] M. F. Rahman, L. Zhong, and K. W. Lim, "An investigation of direct and indirect torque controllers for PM synchronous motor drivers," in *Conf. Rec. PEDS'97*, Singapore, May 1997, pp. 519–523.

[64] ——, "A direct torque controlled interior permanent magnet synchronous motor drive incorporating field weakening," in *Conf. Rec. IEEE-IAS Annu. Meeting*, 1997, pp. 67–74.

[65] M. F. Rahman and L. Zhong, "Comparison of torque response of the interior permanent magnet motor under PWM current and direct torque controls," in *Proc. IEEE IECON'99*, vol. 3, 1999, pp. 1464–1470.

[66] M. F. Rahman, L. Zhong, K. W. Lim, and M. A. Rahman, "A direct torque controlled permanent magnet synchronous motor drive without a sped sensor," in *Proc. Electric Machines and Drives Conf. (IEMD'99)*, May 1999, pp. 123–125.

[67] M. F. Rahman, L. Zhong, M. A. Rahman, and K. Q. Liu, "Voltage switching strategies for the direct torque control of interior magnet synchronous motor drives," in *Proc. ICEM'98*, 1998, pp. 1385–1389.

[68] K. Rajashekara, A. Kawamura, and K. Matsue, *Sensorless Control of AC Motor Drives*. New York: IEEE Press, 1996.

[69] T. Skrotzki, "Die Stromrichtergespeiste Induktionmaschine mit Direkter-Selbstregelung im Feldschwächbereich," Ph.D. thesis, Ruhr-Univ. Bochum, Bochum, Germany, 1989.

[70] A. Steimel and J. Wiesemann, "Further development of direct self control for application in electric traction," in *Proc. IEEE ISIE'96*, Warsaw, Poland, 1996, pp. 180–185.

[71] I. Takahashi and T. Noguchi, "A new quick-response and high efficiency control strategy of an induction machine," *IEEE Trans. Ind. Applicat.*, vol. IA-22, pp. 820–827, Sept./Oct. 1986.

[72] L. Tang, L. Zhong, and F. Rahman, "Modeling and experimental approach of a novel direct torque control scheme for interior permanent magnet synchronous machine drive," in *Proc. IEEE IECON'02*, vol. 1, Seville, Spain, Nov. 2002, pp. 235–240.

[73] D. G. Taylor, "Nonlinear control of electric machines: An overview," *IEEE Contr. Syst. Mag.*, vol. 14, pp. 41–51, Dec. 1994.

[74] D. Telford, M. W. Dunningan, and B. W. Williams, "A comparison of vector control and direct torque control of an induction machine," in *Proc. IEEE PESC'00*, 2000, pp. 421–426.

[75] C. Tian and Y. W. Hu, "Research on the direct torque control in electromagnetic synchronous motor drive," in *Proc. IPEMC 2000, Third Int. Power Electronics and Motion Control Conf.*, vol. 3, pp. 1262–1265.

[76] P. Tiitinen, P. Pohjalainen, and J. Lalu, "Next generation motion control method: Direct torque control (DTC)," *EPE J.*, vol. 5, no. 1, pp. 14–18, Mar. 1995.

[77] A. M. Trzynadlowski, *Control of Induction Motors*. San Diego, CA: Academic, 2000.

[78] P. Vas, *Artificial-Intelligence-Based Electrical Machines and Drives*. New York: Oxford Univ. Press, 1999.

[79] ——, *Sensorles Vector and Direct Torque Control*. Oxford, U.K.: Clarendon, 1998.

[80] A. M. Walczyna, "On reduction of harmonic reactive distortions and subharmonics of drives with VSI-fed induction motors controlled by direct torque and flux control methods," in *Proc. IEEE PESC'95*, Atlanta, GA, 1995, pp. 408–414.

[81] A. M. Walczyna and R. J. Hill, "Novel PWM strategy for direct self-control of inverter-fed induction motors," in *Proc. ISIE Conf.*, Budapest, Hungary, June 1993, pp. 610–615.

[82] J. K. Wang, D. W. Chung, and S. K. Sul, "Direct torque control of induction machine with variable amplitude control of flux and torque hysteresis bands," in *Proc. Int. Conf. Electrical Machines and Drives*, 1999, pp. 640–642.

[83] Y. Xia and W. Oghanna, "Fuzzy direct torque control of induction motor with stator flux estimation compensation," in *Proc. IEEE IECON'97*, vol. 2, 1997, pp. 505–510.

[84] L. Xu and M. Fu, "A novel sensorless control technique for permanent magnet synchronous motors (PMSM) using digital signal processor (DSP)," in *Proc. NEACON'97*, Dayton, OH, July 14–17, 1997, pp. 403–406.

[85] ——, "A sensorless direct torque control technique for permanent magnet synchronous motors," in *Conf. Rec. IEEE-IAS Annu. Meeting*, vol. 1, 1999, pp. 159–164.
[86] ——, "A sensorless direct torque control technique for permanent magnet synchronous motors," in *Power Electronics in Transportation*, Oct. 22–23, 1998, pp. 21–28.
[87] L. Xu, M. Fu, and L. Zhen. A DSP based servo system using permanent magnet synchronous motors (PMSM). Texas Instruments. [Online] Available: http://www.ti.com/
[88] X. Xue, X. Xu, T. G. Habetler, and D. M. Divan, "A low cost stator flux oriented voltage source variable speed drive," in *Conf. Rec. IEEE-IAS Annu. Meeting*, vol. 1, 1990, pp. 410–415.
[89] H. Yuwen, T. Cun, G. Yikang, Y. Zhiqing, L. X. Tang, and M. F. Rahman, "In-depth research on direct torque control of permanent magnet synchronous motor," in *Proc. IEEE IECON'02*, vol. 2, Seville, Spain, Nov. 2002, pp. 1060–1065.
[90] L. Zhong, M. F. Rahman, W. Y. Hu, and K. W. Lim, "Analysis of direct torque control in permanent magnet synchronous motor drives," *IEEE Trans. Power Electron.*, vol. 12, pp. 528–536, May 1998.
[91] M. R. Zolghadri and D. Roye, "Sensorless direct torque control of synchronous motor drive," in *Proc. Int. Conf. Electrical Machines (ICEM'98)*, vol. 2, Istanbul, Turkey, 1998, pp. 1385–1390.
[92] M. R. Zolghadri, J. Guiraud, J. Davoine, and D. Roye, "A DSP direct torque controller for permanent magnet synchronous motor drives," in *Proc. IEEE PESC'98*, vol. 2, 1998, pp. 2055–2061.

Giuseppe S. Buja (M'75–SM'84–F'95) received the Laurea degree in electronic engineering with honors from the University of Padova, Padova, Italy, in 1970.

Upon graduation, he joined the Engineering Faculty of the University of Padova. Since 1986, he has been a Full Professor of Power Electronics, first at the University of Trieste and then at the University of Padova. He has carried out research in the fields of electric energy static converters, electric drives, motion control systems, and fieldbuses, and has authored or coauthored more than 150 papers published in refeered journals and international conference proceedings. He started up the Laboratory of Electric Drives at the University of Trieste and the Laboratory of Industrial Automation at the University of Padova, the latter of which he is currently the Head. He has directed several research projects granted by the university and by private companies.

Prof. Buja has served the IEEE in several capacities, including General Chairman of the 20th Annual Conference of the IEEE Industrial Electronics Society (IEEE IECON'94), Associate Eeditor of the IEEE TRANSACTIONS ON INDUSTRIAL ELECTRONICS, and Vice President of the IEEE Industrial Electronics Society (IES). He was a co-founder of the International Symposium on Diagnostics for Electric Machines, Power Electronics and Drives (SDEMPED). Currently, he is a Senior Member of the Administrative Committee of the IES, a Voted Member of the Executive Council of the Association on Power Electronics and Motion Control (PEMC), and a Member of the General Assembly of the European Power Electronics Association (EPE). He has served as the Coordinator of the Ph.D. course in electrical engineering at the University of Padova. His biography has been included in the last four editions of *Who's Who in the World*.

Marian P. Kazmierkowski (M'89–SM'91–F'98) received the M.S., Ph.D., and Dr. Sci. degrees in electrical engineering from the Institute of Control and Industrial Electronics (ICIE), Warsaw University of Technology, Warsaw, Poland, in 1968, 1972, and 1981, respectively.

From 1967 to 1969, he was with the Industrial Institute of Electrical Engineering, Warsaw-Miedzylesie, Poland, and from 1969 to 1980, he was an Assistant Professor at ICIE. From 1980 to 1983, he was with RWTH Aachen, West Germany, as an Alexander von Humboldt Fellow. From 1986 to 1987, he was a Visiting Professor at NTH Trondheim, Norway. Since 1987, he has been a Professor and Director of ICIE. He was a Visiting Professor at the University of Minnesota, Minneapolis, in 1990, at Aalborg University, Denmark, in 1990 and 1995, and at the University of Padova, Italy, in 1993. He was a Coordinating Professor of the *International Danfoss Professor Program* from 1997 to 2000 at Aalborg University. Since 1996, he has served as an elected member of the State Committee for Scientific Research in Poland. At present, he is also Director of the *Centre of Excellence in Power Electronics and Intelligent Control for Energy Conservation* (European Framework Program V) at ICIE. He is engaged in experimental research and theoretical work on electric drive control and industrial electronics. He is the author or coauthor of over 200 technical papers and reports, as well as 12 books and textbooks. His latest book, coedited with R. Krishnan and F. Blaabjerg, is *Control in Power Electronics* (San Diego, CA: Academic, 2002).

Dr. Kazmierkowski was Chairman of the 1996 IEEE International Symposium on Industrial Electronics held in Warsaw, Poland. He was Vice-President, Publications, of the IEEE Industrial Electronics Society from 1999 to 2001. He is currently Editor-in-Chief of the IEEE TRANSACTIONS ON INDUSTRIAL ELECTRONICS. He has served on several IEEE committees and conference organizing committees. He is Chairman of the IEEE Poland Section.